การปรับปรุงพื้นผิว NiAl-เลเยอร์ดับเบิลไฮดรอกไซด์ ด้วยโดเดกซิลซัลเฟตไอออน เป็นตัวดูดซับสีย้อม

Modification of NiAl-Layered Double Hydroxide with Dodecylsulfate Ion as Dye Adsorbent

ศรชัย อินทะไชย[1*] และ อารีพร เบ้าอุฬาล[2]
Sonchai Intachai[1*] and Areebhorn Baoulan[2]
[1]สาขาเคมี คณะวิทยาศาสตร์ มหาวิทยาลัยทักษิณ
[2]สาขาเคมี คณะวิศวกรรมศาสตร์ มหาวิทยาลัยเทคโนโลยีราชมงคลอีสาน วิทยาเขตขอนแก่น
[1]Department of Chemistry, Faculty of Science, Thaksin University
[2]Department of Chemistry, Faculty of Engineering, Rajamangala University of Technology Isan, Khon Kaen Campus

Received : 9 April 2019
Revised : 30 September 2019
Accepted : 6 October 2019

บทคัดย่อ

งานวิจัยนี้ได้ปรับปรุงพื้นผิว NiAl-เลเยอร์ดับเบิลไฮดรอกไซด์ (NiAl-LDH) ด้วยโดเดกซิลซัลเฟต โดยการทำปฏิกิริยาระหว่างสารละลายโซเดียมโดเดกซิลซัลเฟต (DS^-) และสารแขวนลอย NiAl-LDH ในน้ำ ภายใต้ปฏิกิริยาไฮโดรเทอร์มอลที่อุณหภูมิ 120 องศาเซลเซียส เป็นเวลา 24 ชั่วโมง และปรับเปลี่ยนปริมาณ DS^- ที่ใช้แตกต่างกันโดยจำกัดปริมาณ LDH ซึ่งใช้สัญลักษณ์ตัวห้อย x ในสารผลิตภัณฑ์ DS_x@NiAl-LDH ที่เตรียมได้ จากรูปแบบการเลี้ยวเบนของรังสีเอกซ์ พบว่าช่องว่างระหว่างชั้นของ NiAl-LDH ขยายกว้างขึ้นตามการเพิ่มปริมาณ DS^- จนถึง 3.52 นาโนเมตร ที่ x = 50 ซึ่งแสดงว่าการจัดเรียงตัวของ DS^- ในช่องว่างระหว่างชั้นเป็นแบบ paraffin bilayer จากการศึกษาการกำจัดสีย้อมเมทิลออร์เรนจ์ เมทิลีนบลู และ อะลิซารีน ด้วย DS_{50}@NiAl-LDH จากสารละลาย พบว่า ตัวดูดซับที่ถูกปรับปรุงพื้นผิวมีประสิทธิภาพในการกำจัดเมทิลออร์เรนจ์ได้สูงสุด 97% เนื่องจากอันตรกิริยาทางไฟฟ้าสถิต และยังดูดซับสีย้อมแต่ละชนิดได้ดีกว่า NiAl-LDH บริสุทธิ์ ซึ่งเป็นผลจากแรงดึงดูดไฮโดรโฟบิก และพันธะไฮโดรเจน

คำสำคัญ : NiAl-เลเยอร์ดับเบิลไฮดรอกไซด์, โดเดกซิลซัลเฟต, ตัวดูดซับ, สีย้อม

***Corresponding author.** E-mail : sonchai.i@tsu.ac.th

Abstract

In this work, NiAl-layered double hydroxide (NiAl-LDH) modified with dodecylsulfate was prepared by the reaction between an aqueous solution of dodecylsulfate (DS^-) and an aqueous suspension of NiAl-LDH under hydrothermal reaction at 120 °C for 24 h. Various amounts of DS^- were studied with the controlled amount of the LDH which referred to subscript x in DS_x@NiAl-LDH for the as-prepared products. The XRD patterns of all products revealed that the interlayer space was increased with increasing the amount of DS^- up to 3.52 nm where $x = 50$ owing to the paraffin bilayer arrangement of DS^- molecules in the interlayer space. DS_{50}@NiAl-LDH was used as the representative adsorbent for elimination of methyl orange, methylene blue and alizarin from solution. The modified adsorbent showed the highest removal efficiency of methyl orange at 97% due to the electrostatic interaction. In addition, for every type of dye tested, the adsorption capacity of the surface-modified NiAl-LDH was superior to the pristine NiAl-LDH due to the improved hydrophobic and hydrogen bonding interactions in the former.

Keywords : NiAl-layered double hydroxide, dodecylsulfate, adsorbent, dye

Introduction

Layered inorganic materials have been extensively interested in the roles of host and support materials with hybridizing or compositing an inorganic and/or organic species as a result of the capacity on controlling the growth of nanomaterial, rigid structure and many features such as charged surface, ion exchangeability, large surface area and catalyst (Yang *et al.*, 2019). The processes show the achievement for nanohybrid preparation, which synergized to achieve the environmental purification and production of alternative energy fuels (Mohapatra & Parida, 2016). Based on positively charged layer, $M^{II}M^{III}$-layered double hydroxide (abbreviated as $M^{II}M^{III}$-LDH) is one of the dominant host materials especially as anion exchanger and adsorbent. Structure of the LDH is composed of isomorphic substitution of divalent metal (M^{II}) ions in some sites of M(II) hydroxide nanosheets (brucite-like structure) by trivalent (M^{III}) one, generating the net positive charge on surface and then the solid is formed layer by layer in the presence of counterbalanced anionic (A^{n-}) species and water (H_2O) molecule having general formula of $[M^{III}_xM^{II}_{1-x}(OH)_2]^{x+}\cdot[A^{n-}]_{x/n}\ mH_2O$ (Yang *et al.*, 2019). Two dimensional layered structure of the LDH makes such characteristic properties as capacities of anion exchange and adsorption, swelling ability, large surface area, catalyst and so on. In addition, the diverse of divalent and trivalent cations in the compositions of LDH can be varied that promotes the different and unexpected functionalities such as adsorbent, catalyst, catalyst support, drug deliver and so on (Sun *et al.*, 2015: Mohapatra & Parida, 2016: Kong *et al.*, 2018a). In the present work, NiAl-LDH was used as the host material due to easy preparation with large amount, low cost and high stability.

A big problem of environmental issue is wastewater contaminated by industrial and agricultural chemicals, and so forth. One of these effluents consists of organic dye molecules mostly originated from industries relating to textile (handicraft), paints, cosmetics, food and so forth. Menacingly, dye can be toxic (mutagenicity, genotoxicity, etc.) and carcinogenic even in tiny amount. The quality of water is an important factor on health, consequently, the removal of dyes and other organic contaminants from water resources is a task of the utmost importance for researchers. Conventionally, purification process of wastewater is transferring dye molecules onto a solid adsorbent, however, the adsorbent must be rigid and versatile for all species of dye molecules. Especially, methyl orange, methylene blue and alizarin are the representative of anionic, cationic and neutral dyes, which difficult to degrade because of high stabilities of their structure (Scheme 1). Adsorption process using positively charged–layered inorganic adsorbent shows efficient removal of negatively charged dye in wastewater with the electrostatic interaction, however, the species that contaminated are molecules of different charge like negative, positive and/or neutral. Therefore, the adsorbent is needed to modify for multipurpose adsorption of various charge–dye molecules. The modification of layered materials with surfactants as organo–adsorbent has been investigated so far and the tailor of removal efficiency of dye from solution was obtained (Sun *et al.*, 2015: Kong *et al.*, 2018a). Besides, thermal stability and flame retardancy of polymer/intumescent flame retardant are improved by the protection of NiAl–LDH modified with dodecylsulfate (Kong *et al.*, 2018b). As we known, the intercalation of dodecylsulfate in the interlayer space of NiAl–LDH under hydrothermal reaction as the adsorbent for eliminating dye (methyl orange, methylene blue and alizarin) molecules from solution has not been studied so far. It may be thought that the enlargement of the interlayer space with surfactant may accommodate the toxic species more with many attractive forces. *Herein*, the intercalation of dodecylsulfate in the interlayer space of NiAl–LDH was investigated by hydrothermal method, and the difference in the loading amounts of dodecylsulfate was also studied. Furthermore, the modified NiAl–LDH was examined removal efficiency of various dye molecules in solution.

Methods

Materials

Hydrated salts of nickel chloride ($NiCl_2 \cdot 6H_2O$) and aluminium chloride ($AlCl_3 \cdot 6H_2O$) were purchased from Carlo Erba Reagenti. Urea ($(NH_2)_2CO$) was purchased from Asia Pacific Specialty Chemicals LTD. Sodium dodecylsulfate ($NaC_{12}H_{25}SO_4$) was purchased from Ajax Finechem Pty LTD. Methyl orange ($C_{14}H_{14}N_3NaO_3S$), methylene blue ($C_{16}H_{18}ClN_3S$) and alizarin ($C_{14}H_8O_4$) were purchased from Acros. All chemicals are the reagent grade and were used directly without any further purification.

Synthesis of NiAl–LDH and DS$_x$@NiAl–LDH

NiAl–LDH was prepared by hydrothermal method using urea hydrolysis (pH 9.0 ± 0.5). An aqueous solution of metal chlorides containing $NiCl_2$ (10 mM) and $AlCl_3$ (5 mM), and an aqueous solution of $(NH_2)_2CO$ (35 mM) were mixed under magnetic stirring for 10 min. Then, the as-prepared solution was transferred into Teflon–line autoclave and hydrothermally treated at 150 °C for 48 h. The apple green colored solid due to NiAl–LDH was obtained by centrifugation, washed several times with deionized (DI) water, and then ethanol, finally dried at 60 °C for 24 h. The modification of NiAl–LDH with dodecylsulfate (DS^{-}) was carried out by the reaction of an aqueous solution of sodium dodecylsulfate (SDS) and the aqueous suspension of NiAl–LDH under magnetic stirring for 10 min, and then transferred into Teflon–line autoclave at hydrothermally heating of 120 °C for 24 h. The loading amount of DS^{-} was varied by 20, 30, 40 and 50 times of the theoretical anion exchange capacity (AEC) where it is about 300 meq/100 g of the LDH. The modified NiAl–LDH powder was isolated by centrifugation, and then washed several times with DI water and then ethanol, finally dried at 60 °C for 24 h. The obtained products were abbreviated as DS_x@NiAl–LDHs, where subscript x was referred to the ratio of DS^{-} amount to the AEC.

Adsorption of dye solution

To assess the potential ability of the modified NiAl–LDH in comparison with pristine NiAl–LDH in wastewater treatment, the adsorption rate of methyl orange, methylene blue and alizarin molecules on DS_{50}@NiAl–LDH was evaluated at room temperature in the dark area. Each 50 mL dye solution with 20 ppm concentration and 15 mg of adsorbent powder were added in beaker (150 mL) under magnetically stirring for 3 h in the dark. The aliquot parts of the residual solution without adsorption were collected every 30 min until 3 h to examine the removal efficiency by using UV–visible spectrophotometer followed as the eq. 1.

$$\text{Removal efficiency (\%)} = ((C_i - C_t)/C_i) \times 100 \qquad (1)$$

Where C_i (mg/L) and C_t (mg/L) are the dye concentration at initial (no adsorbent) and any (t) time (min).

Characterization

Powder X–ray diffraction (XRD) patterns were measured on a Bruker D8 ADVANCE diffractometer using monochromatic CuKα radiation with λ = 1.5418 Å operated at 40 kV and 40 mA. The data were collected at the scanning rate of 0.5 degree per minute over the region of 2–50 degrees. Fourier transform infrared spectra of the samples were recorded on a Perkin Elmer Spectrum One FT–IR spectrophotometer by KBr disk method. Thermogravimetric–differential thermal (TG–DTA) curves were recorded on Perkin Elmer Pyris Diamond TG–DTA instrument under a dry air flow at a heating rate of 10 °C min^{-1} using α–alumina (α–Al_2O_3) as the standard material. Diffuse reflectance absorption (UV–visible) spectra of the solid samples in the range of 200–800 nm were carried out on a Shimadzu UV–VIS–NIR3101PC scanning spectrophotometer using an integrated sphere. UV–visible absorption spectra of the dye solutions were conducted in the wavelength range of 200–800 nm using a Shimadzu UV–1700 Pharmaspec UV–VIS spectrophotometer.

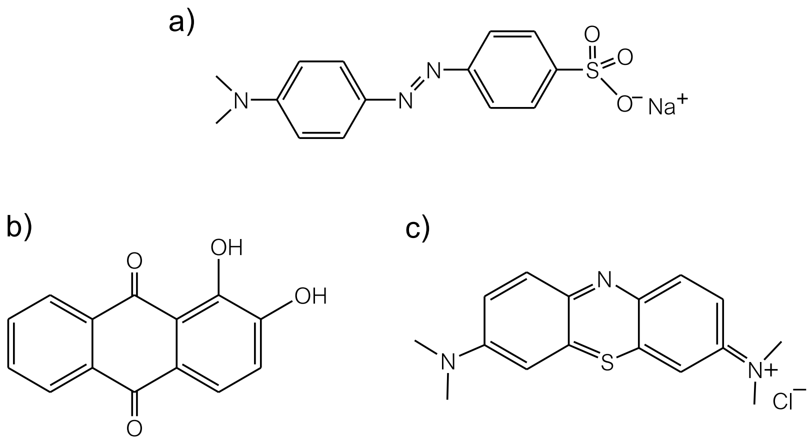

Scheme 1 Dye structures of methyl orange (a), alizarin (b) and methylene blue (c)

Table 1 Basal spacing, interlayer expansion and/or absorption bands of all products

Product	Basal spacing (d_{003}) due to DS$^-$ (nm)	Interlayer expansion due to DS$^-$ (nm)	λ_{abs} (nm), $^3A_{2g} \rightarrow {}^3T_{1g}(P)$	λ_{abs} (nm), $^3A_{2g} \rightarrow {}^3T_{1g}(F)$
DS$_{50}$@NiAl–LDH	4.00	3.52	379	655
DS$_{40}$@NiAl–LDH	2.96	2.48	379	655
DS$_{30}$@NiAl–LDH	2.96	2.48	379	655
DS$_{20}$@NiAl–LDH	–	–	379	655
pristine NiAl–LDH	–	–	377	650

Results

The XRD patterns of DS$_x$@NiAl–LDHs and pristine NiAl–LDH are shown in Figure 1. The XRD pattern of pristine NiAl–LDH (Figure 1e) showed the (*003*) reflections with the basal spacing (d_{003}) of *ca.* 0.8 nm that are a characteristic crystal plane of hydrotalcite–like structure (JCPDS No. 22–0452) together with the presence of CO_3^{2-} ion in the interlayer space. So the d_{003} about 0.8 nm for the products with x = 20–40 was corresponding to CO_3^{2-} intercalated in the interlayer space. After the modification of NiAl–LDH with DS$^-$ ion under hydrothermal reaction, the XRD patterns of the products with x = 30–50 were changed significantly, meanwhile the XRD pattern of DS$_{20}$@NiAl–LDH was nearly similar to that of NiAl–LDH. This result interpreted that the amount of DS$^-$ was important role on achieving the intercalation with substitution of CO_3^{2-} ions in the interlayer space. It was clearly seen as increasing the loading amount of DS$^-$ (x = 30–40), the additional XRD peaks were appeared at lower position of 2θ = *ca.* 7° and 3° on which were (*006*) and (*003*) reflections, respectively, meanwhile the XRD peaks of DS$_{50}$@NiAl–LDH due to (*003*), (*006*) and (*009*) reflections (Figure 1a) were shifted to lower 2θ position (Ogawa & Hiramine, 2014: Kong *et al.*, 2018a).

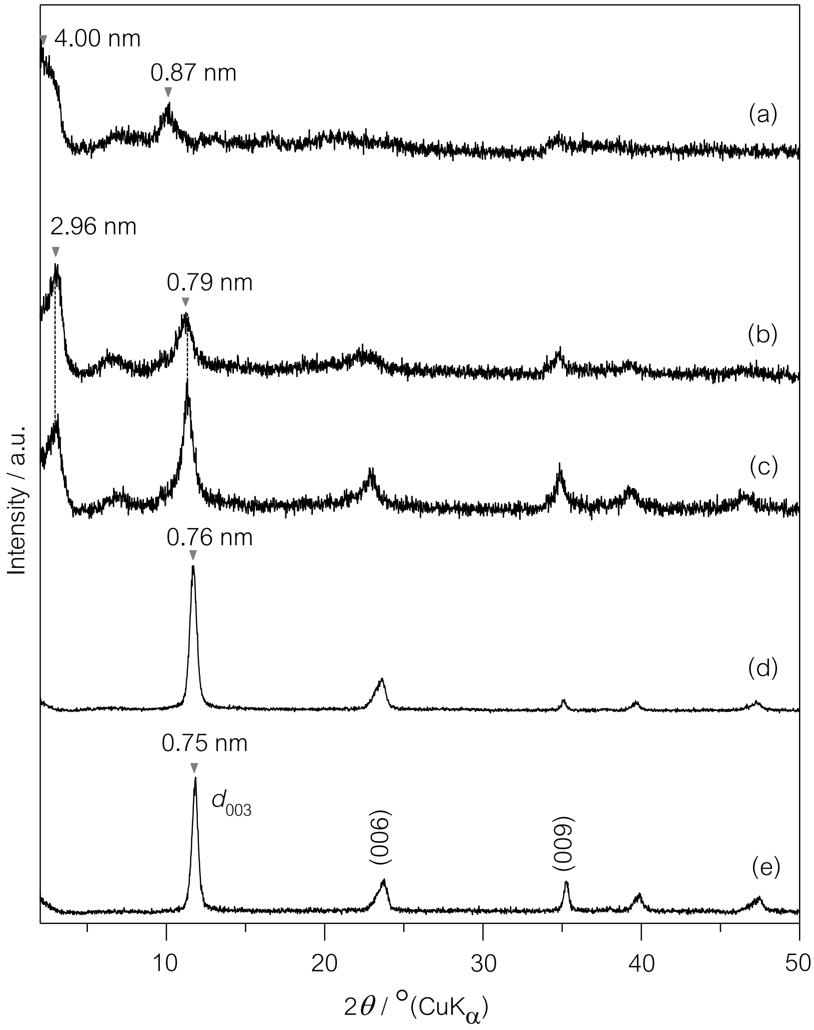

Figure 1 XRD patterns of DS_{50}@NiAl–LDH (a), DS_{40}@NiAl–LDH (b), DS_{30}@NiAl–LDH (c), DS_{20}@NiAl–LDH (d) and pristine NiAl–LDH (e)

By subtracting the thickness of the LDH nanosheet (0.48 nm) from the d_{003} (2.96, 2.96 and 4.00 nm) that calculated from Bragg's equation, the interlayer space of the products was expanded to be 2.48, 2.48 and 3.52 nm for DS_{30}@NiAl–LDH, DS_{40}@NiAl–LDH and DS_{50}@NiAl–LDH, respectively (Table 1). This confirmed the intercalation of DS^- in the interlayer space of the LDH, besides all CO_3^{2-} ions in the interlayer space of DS_{50}@NiAl–LDH were eliminated with the substitution by DS^- ions corresponding to the FTIR result (discussed later).

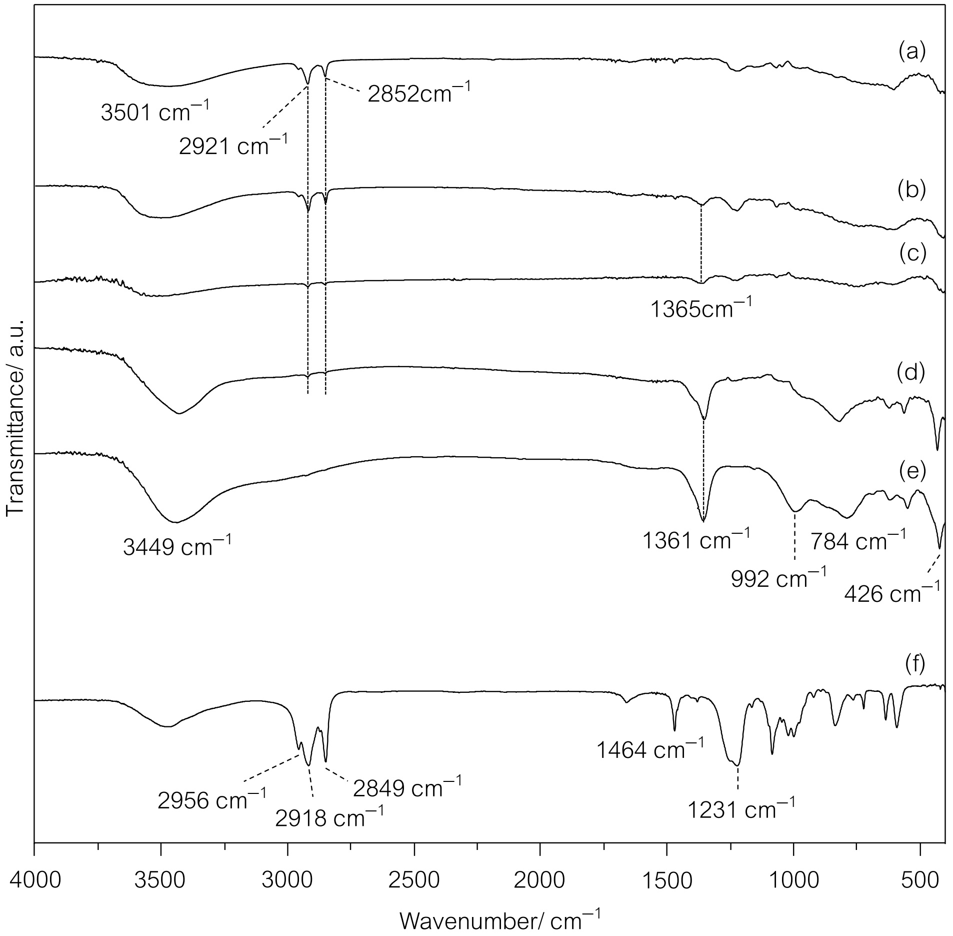

Figure 2 FTIR spectra of DS_{50}@NiAl–LDH (a), DS_{40}@NiAl–LDH (b), DS_{30}@NiAl–LDH (c) DS_{20}@NiAl–LDH (d), pristine NiAl–LDH (e) and sodium dodecylsulfate (SDS) (f)

To confirm the presence of DS^{-} ions in the products and the substitution of CO_3^{2-} ions that counterbalanced in the interlayer space, the FTIR spectra of all products together with NiAl–LDH and SDS were investigated (Figure 2). All FTIR bands of NiAl–LDH (Figure 2e) were according to the hydrotalcite–like structure of the LDH in the presence of CO_3^{2-} ion with the characteristic band at 1361 cm^{-1} (Liu *et al.*, 2006: Zhang *et al.*, 2014). The FTIR bands of all products reveled the asymmetric and symmetric CH_2 stretching vibrations at 2921 and 2852 cm^{-1}, respectively (Liu *et al.*, 2006), and these observed bands were shifted to higher frequency in comparison with those of pure SDS (at 2918 and 2849 cm^{-1}, Figure 2f). The FTIR result indicated the presence of DS^{-} in the hybrids, meanwhile, the decarbonation from the interlayer space was also occurred with gradual disappearance of the FTIR band at 1361 cm^{-1} due to CO_3^{2-} as increasing the loading amount of DS^{-} up to 50 times of the AEC (DS_{50}@NiAl–LDH) where that band was vanished (Figure 2a) that could confirm the success of the intercalation of DS^{-}.

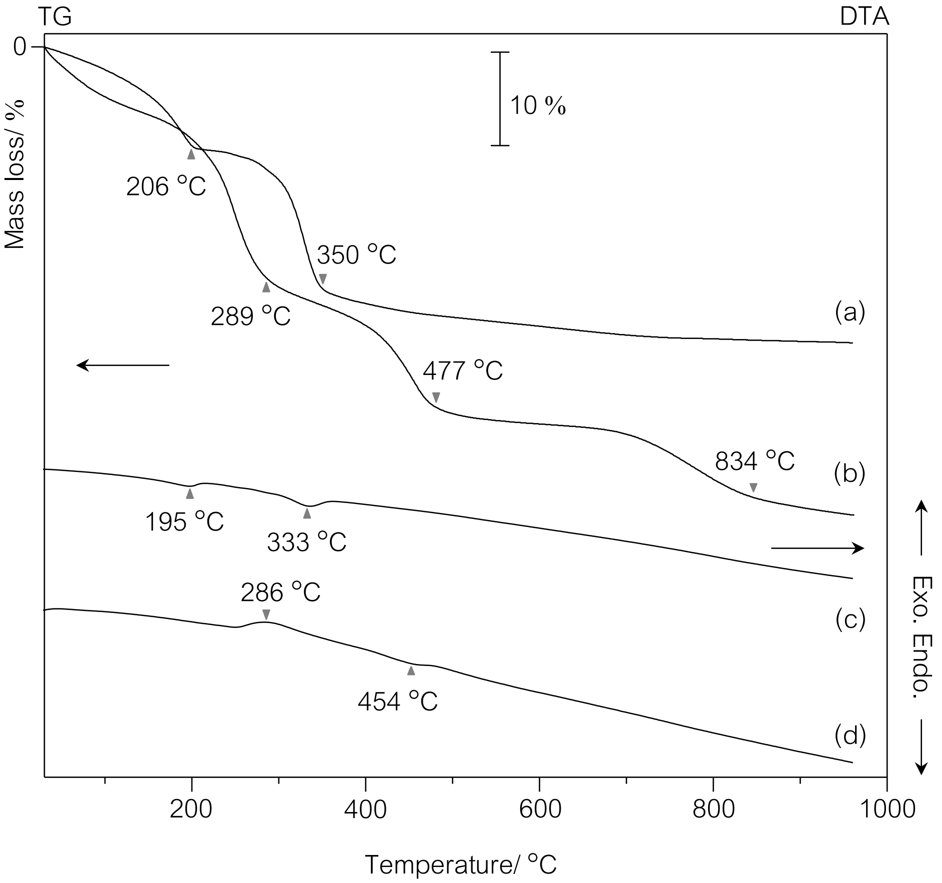

Figure 3 TG–DTA curves of pristine NiAl–LDH (a, c) and DS_{50}@NiAl–LDH (b, d)

Figure 3 shows TG–DTA curves of DS_{50}@NiAl–LDH and NiAl–LDH. The thermal behavior of NiAl–LDH displayed two stages of mass loss. The first mass loss stage (Figure 3a) took place from room temperature up to 206 °C corresponding to the endothermic DTA peak at 195 °C (Figure 3c), interpreting to the evaporation of surface and interlayer water molecules and the partial elimination of CO_2 molecules (from intercalated CO_3^{2-}), respectively. The second mass loss stage occurred from 206 °C to 350 °C that associated with the endothermic DTA peak at 333 °C, indicating to the decomposition of the intercalated CO_3^{2-} and the dehydroxylation of brucite–like layers as CO_2 and water molecules, respectively. Meanwhile, the TG curve of DS_{50}@NiAl–LDH was divided into 4 stages. The first one of mass loss showed the same thermal behavior in that of NiAl–LDH. The latter mass loss stage occurred from 206 °C to 289 °C was attributed to the removal of the organic species (the intercalated DS^- molecule), supporting to the exothermic DTA peak at 286 °C due to the formation of SO_2 molecule. The third mass loss stage was appeared between 289 °C and 477 °C that corresponded to the endothermic DTA peak at 454 °C assigning to the dehydroxylation of the LDH sheets. The last stage of mass loss above 477 °C was due to further decomposition of the intercalated DS^- molecules and occurrence of dehydroxylation. This result could further confirm the presence of DS^- in the hybrids.

The diffuse reflectance absorption spectra were also investigated for understanding the optical property of the products in comparison with NiAl–LDH as shown in Figure 4. The absorption spectrum of pristine NiAl–LDH displayed two characteristic absorption bands due to d–d transition of Ni^{2+} ions (Figure 4e). The first absorption band was observed at *ca*. 380 nm attributing to the $^3A_{2g}(F) \rightarrow {}^3T_{1g}(P)$ transition, and the second one was located at *ca*. 650 nm corresponding to the $^3A_{2g}(F) \rightarrow {}^3T_{1g}(F)$ transition (Wang *et al*., 2010). As characterized, the absorption spectra of all products showed the similar d–d transitions to those of NiAl–LDH. All of the data are listed in Table 1. However, the intercalation of DS^- in the interlayer space of NiAl–LDH slightly differentiated the electronic spectrum of the LDH with extending the absorption wavelength from 377 nm to 379 nm and that from 650 nm to 655 nm, and promoting the increment of the light absorption as increasing the loading amount of DS^-. This results might be due to the host–guest interaction (Ontam *et al*., 2012).

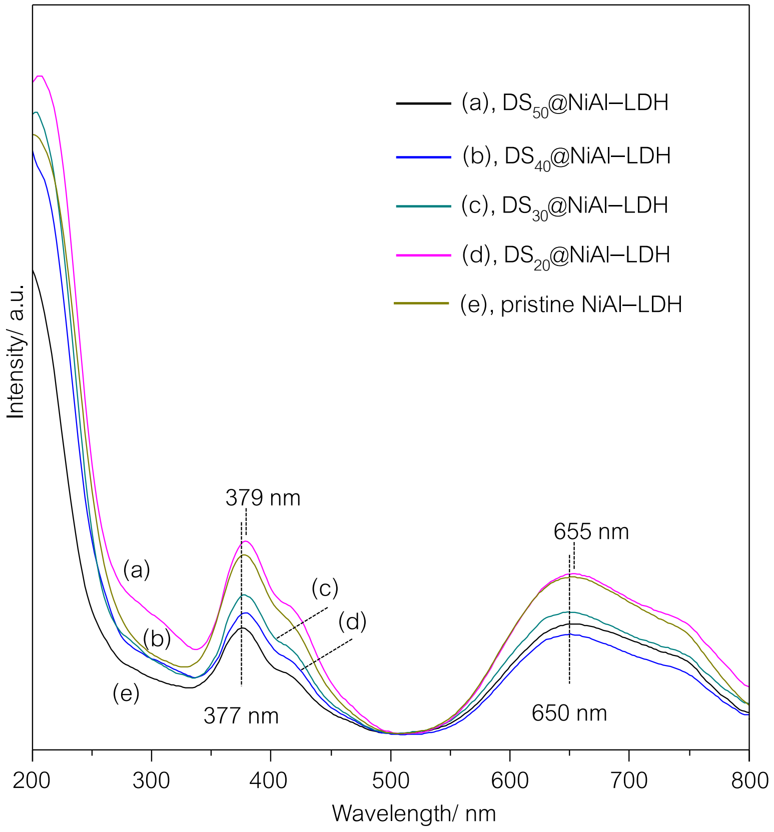

Figure 4 UV–visible spectra of DS_{50}@NiAl–LDH (a), DS_{40}@NiAl–LDH (b), DS_{30}@NiAl–LDH (c) DS_{20}@NiAl–LDH (d), and pristine NiAl–LDH (e)

The removal efficiency of dye molecules with various charge of methyl orange, methylene blue and alizarin, was examined by using DS_{50}@NiAl–LDH as the representative of the adsorbents due to the largest interlayer space and the absence of CO_3^{2-} ion. After the adsorption process was reached the equilibrium within 60 min, the methyl orange molecules were mostly adsorbed by 97%, meanwhile, alizarin and methylene blue molecules were removed by just 35% and 24%, respectively (Figure 5). In comparison with pristine NiAl–LDH, the adsorption ability of DS_{50}@NiAl–LDH was superior for the adsorption of each dye that resulted from the hydrophobic and hydrogen bonding interactions. However, NiAl–LDH adsorbent showed the removal efficiency of methyl orange about 2.0–2.5 times compared to that of methylene blue and alizarin using DS_{50}@NiAl–LDH adsorbent. This result indicated that the electrostatic attraction was more important factor than either the hydrophobic interaction or hydrogen bonding.

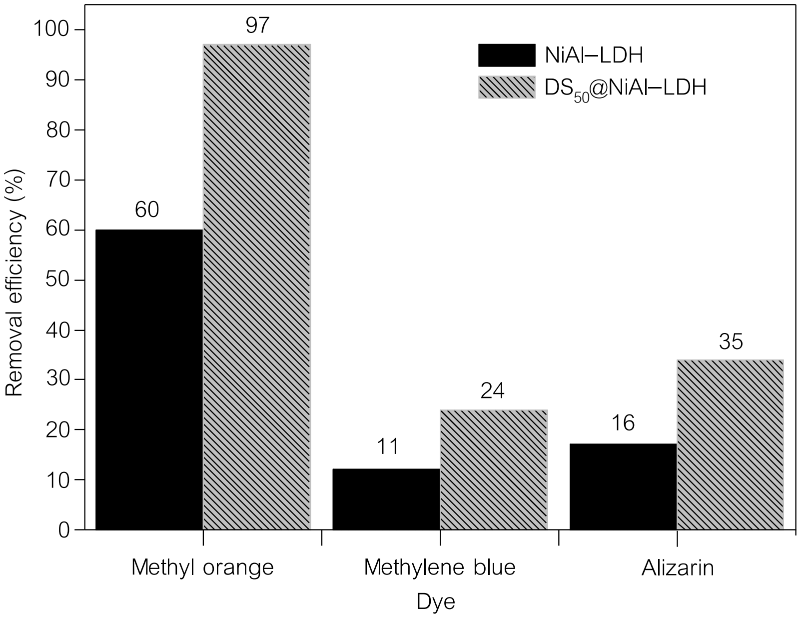

Figure 5 Removal efficiency of various dye molecules by using DS_{50}@NiAl–LDH as adsorbent

Discussion

From the XRD and FTIR results, the loading amount of DS^- with x = 20 was inadequate to substitute the intercalated CO_3^{2-} and/or some molecules were bonded on lateral sites of the nanosheets, and for the products with x = 30–40 the CO_3^{2-} ions were still accommodated in the interlayer space together with DS^- molecules due to the segregation (Ogawa & Hiramine, 2014). Taking the expansion of the interlayer space (3.52 nm for DS_{50}@NiAl–LDH) and the length of DS^- (2.08 nm) (Kong *et al.*, 2018a), the DS^- molecules were arranged with paraffin bilayer (Damel *et al.*, 2014) as shown in Scheme 2. For studying the removal efficiency of various dye species from solution, the organo–adsorbent, DS_{50}@NiAl–LDH showed the most elimination of methyl orange in comparison with alizarin and methylene blue. It was as a result of the attractive force between negatively charged methyl orange molecule (Scheme 1) and positively charged layer of the adsorbent, as well as the other forces for three dye molecules was the hydrophobic interaction of the hydrophobic part between the intercalated DS^- long-chain tail and aromatic group of the dye, and hydrogen bonding interaction, namely, guest-guest and host-guest interactions in the interlayer space (Kong *et al.*, 2018a). As a result, the modification of NiAl–LDH with dodecylsulfate (50 times of the AEC) promoted the enhanced removal efficiency of dye molecules.

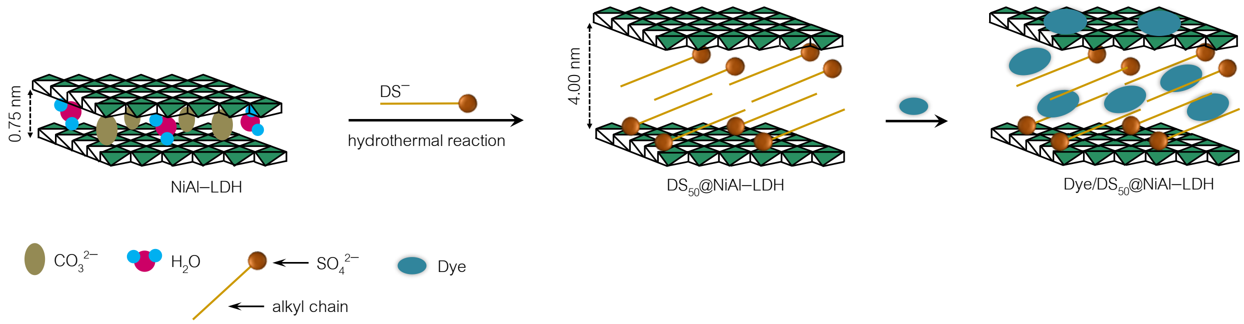

Scheme 2 Intercalation of dodecylsulfate (DS^-) and adsorption mechanism of dye molecules

Conclusions

The surface modification of NiAl-layered double hydroxide with dodecylsulfate had been carried out using hydrothermal reaction at 120 °C for 24 h. The XRD, FTIR and TG-DTA results confirmed the intercalation of dodecylsulfate in the interlayer space of NiAl–LDH and the substitution of CO_3^{2-} ions was completed by adjusting the amount of dodecylsulfate to be 50 times of the anion exchange capacity of the LDH. DS_{50}@NiAl–LDH exhibited the highest removal efficiency of methyl orange from solution when compared to the adsorption of methylene blue and alizarin. The result was due to the electrostatic force between negative charge-methyl orange dye and positive-charge surface of the adsorbent and the hydrophobic interaction between long-chain tail of the intercalated dodecylsulfate molecules and aromatic group of dye in the larger nanospace of the hybrid.

Acknowledgements

We gratefully acknowledge Department of Chemistry, Faculty of Science, Thaksin University, Phatthalung for providing materials, equipment and facilities. This work was supported by Thaksin University Research Fund, Thailand.

References

Demel, J., Hynek, J., Kovář, P., Dai, Y., Taviot–Guého, C., Demel, O., Pospíšil, M. & Lang, K. (2014). Insight into the structure of layered zinc hydroxide salts intercalated with dodecyl sulfate anions. *The Journal of Physical Chemistry C*, *118*, 27131–27141.

Kong, Y., Huang, Y., Meng, C. & Zhang, Z. (2018a). Sodium dodecylsulfate–layered double hydroxide and its use in the adsorption of 17β–estradiol in wastewater. *RSC Advances*, *8*, 31440–31454.

Kong, Q., Wu, T., Wang, J., Liu, H. & Zhang, J. (2018b). Improving the thermal stability and flame retardancy of PP/IFR composites by NiAl–layered double hydroxide. *Journal of Nanoscience and Nanotechnology*, *18*, 3660–3665.

Liu, Z., Ma, R., Osada, M., Iyi, N., Ebina, Y., Takada, K. & Sasaki, T. (2006). Synthesis, anion exchange, and delamination of Co–Al layered double hydroxide: Assembly of the exfoliated nanosheet/polyanion composite films and magneto–optical studies. *Journal of the American Chemical Society*, *128*, 4872–4880.

Ogawa, M. & Hiramine, M. (2014). Direct correlation between nanostructure and particle morphology during intercalation. *Crystal Growth & Design*, *14,* 1516–1519.

Ontam, A., Khaorapapong, N. & Ogawa, M. (2012). Immobilization of cadmium telluride nanoparticles on the surface of hexadecyltrimethylammonium–montmorillonite. *Journal of Materials Chemistry*, *22*, 20001–20007.

Sun, Y., Zhou, J., Cai, W., Zhao, R. & Yuan, J. (2015). Hierarchically porous NiAl–LDH nanoparticles as highly efficient adsorbent for p–nitrophenol from water*. Applied Surface Science*, *349*, 897–903.

Wang, H., Xiang, X. & Li, F. (2010). Facile synthesis and novel electrocatalytic performance of nanostructured Ni–Al layered double hydroxide/carbon nanotube composites. *Journal of Materials Chemistry*, *20,* 3944–3952.

Yang, Z.–Z., Wei, J.–J., Zeng, G.–M., Zhang, H.–Q., Tan, X.–F., Ma, C., Li, X.–C., Li, Z.–H. & Zhang, C. (2019). A review on strategies to LDH–based materials to improve adsorption capacity and photoreduction efficiency for CO_2. *Coordination Chemistry Reviews*, *386*, 154–182.

Zhang, C., Yang, S., Chen, H., He, H. & Sun, C. (2014). Adsorption behavior and mechanism of reactive brilliant red X–3B in aqueous solution over three kinds of hydrotalcite–like LDHs. *Applied Surface Science*, *301,* 329–337.